Accepted Manuscript

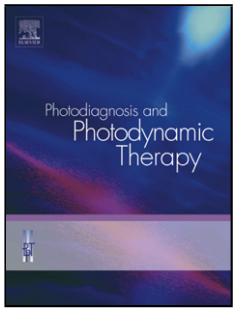

Title: The effect of indocyanine green loaded on a novel nano-graphene oxide for high performance of photodynamic therapy against *Enterococcus faecalis*

Authors: Tayebeh Akbari, Maryam Pourhajibagher, Farzaneh Hosseini, Nasim Chiniforush, Elham Gholibegloo, Mehdi Khoobi, Sima Shahabi, Abbas Bahador

PII: S1572-1000(17)30429-5
DOI: http://dx.doi.org/10.1016/j.pdpdt.2017.08.017
Reference: PDPDT 1014

To appear in: *Photodiagnosis and Photodynamic Therapy*

Received date: 21-6-2017
Revised date: 13-8-2017
Accepted date: 15-8-2017

Please cite this article as: Akbari Tayebeh, Pourhajibagher Maryam, Hosseini Farzaneh, Chiniforush Nasim, Gholibegloo Elham, Khoobi Mehdi, Shahabi Sima, Bahador Abbas.The effect of indocyanine green loaded on a novel nano-graphene oxide for high performance of photodynamic therapy against Enterococcus faecalis.*Photodiagnosis and Photodynamic Therapy* http://dx.doi.org/10.1016/j.pdpdt.2017.08.017

The effect of indocyanine green loaded on a novel nano-graphene oxide for high performance of photodynamic therapy against *Enterococcus faecalis*

Running title: PDT effect of novel nano-graphene oxide containing ICG against *E. faecalis*

Tayebeh Akbari[1], Maryam Pourhajibagher[2,3,4], Farzaneh Hosseini[1], Nasim Chiniforush[3], Elham Gholibegloo[5,6], Mehdi Khoobi[6,7], Sima Shahabi[3,8], Abbas Bahador[3,4,9]*

[1]Department of Microbiology, Islamic Azad University, North Tehran Branch, Theran, Iran.
[2]Dental Implant Research Center, Dentistry Research Institute, Tehran University of Medical Sciences, Tehran, Iran.
[3]Laser Research Center of Dentistry (LRCD), Dentistry Research Institute, Tehran University of Medical Sciences, Tehran, Iran.
[4]Dental Research Center, Dentistry Research Institute, Tehran University of Medical Sciences, Tehran, Iran.
[5]Department of Chemistry, Faculty of Science, University of Zanjan, Zanjan, Iran.
[6]Nanobiomaterials Group, Pharmaceutical Sciences Research Center, Tehran University of Medical Sciences, Tehran, Iran
[7]Department of Pharmaceutical Biomaterials and Medical Biomaterials Research Center, Faculty of Pharmacy, Tehran University of Medical Sciences, Tehran, Iran.
[8]Research Center for Science and Technology in Medicine, Tehran University of Medical Sciences, Tehran, Iran.
[9]Department of Microbiology, School of Medicine, Tehran University of Medical Sciences, Tehran, Iran.

***Corresponding author:**
Abbas Bahador, Ph.D., Department of Microbiology, School of Medicine, Tehran University of Medical Sciences, Keshavarz Blvd, 100 Poursina Ave., Tehran, Iran. 14167-53955. Tel.: +9821 6405 3210; Fax: +98218895 5810. E-mail: abahador@sina.tums.ac.ir ; alternate address: ab.bahador@gmail.com.

Highlights:

- Nano-Graghene oxide (NGO) as a novel platform of conjugation of indocyanine green (ICG) can enhance antimicrobial photodynamic therapy (aPDT).
- NGO-ICG-PDT significantly reduced cell viability of *E. faecalis* by 2.81-log as compared to the control group (untreated bacteria; all $P < 0.05$).
- A 99.4% reduction was observed in biofilm formation ability of *E. faecalis* in NGO-ICG-PDT as compared to the control group ($P < 0.05$).
- NGO-ICG-PDT antimicrobial activity against *E. faecalis* at lower ICG concentrations (200 μg/mL) was 47% more than ICG-PDT (1000 μg/mL) ($P<0.05$)
- NGO-ICG-PDT anti-biofilm activity against *E. faecalis* at lower ICG concentrations (200 μg/mL) was 1.3 time more than ICG-PDT (1000 μg/mL, $P > 0.05$)

Abstract

Background: Recently developed photodynamic therapy (PDT) has gained attention for achieving effective root canal disinfection. Using an optimized nontoxic photosensitizer (PS), such as indocyanine green (ICG), is an imperative part of this technique. Therefore, the objective of the current study was to improve ICG photodynamic properties through incorporation of ICG into nano-graphene oxide (NGO) in order to produce NGO-ICG as a new PS and also to assess the antimicrobial effects of NGO-ICG against *Enterococcus faecalis* after photodynamic therapy.

Materials and methods: NGO-ICG was synthesized based on oxidation of graphite flakes and direct loading of ICG onto NGO. NGO-ICG formation was confirmed using the Fourier Transform Infrared Spectroscopy (FT-IR), Scanning Electron Microscopy (SEM), and UV–Vis spectrometry. The antimicrobial and anti-biofilm potential of NGO-ICG against *E. faecalis* was assessed via colony forming unit and crystal violet assays, respectively.
Results: FT-IR, SEM and UV–vis spectrometry confirmed successful synthesis of NGO-ICG containing 200 μg/mL of ICG. NGO-ICG-PDT at an energy density of 31.2 J/cm^2 showed a significant reduction (2.81 log) in the count of *E. faecalis* ($P < 0.05$). NGO-ICG-PDT significantly reduced the biofilm formation ability of *E. faecalis* up to 99.4% ($P < 0.05$). The overall antimicrobial and anti-biofilm potential of NGO-ICG-PDT was higher than PDT based on ICG (1000 μg/mL) (47% and 21%, respectively).
Conclusion: Because NGO-ICG-PDT showed a significant reduction in the number and biofilm formation ability of *E. faecalis* at low ICG concentrations (200 μg/mL), it could be a new approach to adjuvant treatment of endodontic infections.

Keywords: biofilm, *Enterococcus faecalis*, indocyanine green, nano-graphene oxide, photodynamic therapy

1. Introduction

One part of endodontic infection treatment is the management of microorganisms and their by-products, which targets the microorganisms residing inside the infected root canal system [1]. The complexity of the root canal system and increased bacterial resistance make it practically impossible to completely remove microorganisms from infected root canals through instrumentation, irrigation, and intracanal medicaments [1-3].

Enterococcus faecalis, a facultative anaerobic Gram-positive coccus, is one of the most predominant bacteria isolated from root canals after endodontic failure [4]. Reports show that *E. faecalis* is resistant to common antimicrobial irrigants such as sodium hypochlorite, calcium hydroxide, and chlorhexidine due to biofilm formation [5]. Evidence shows that bacteria in biofilm matrices are more resistant (up to 1000 times more resistant) to antimicrobial agents when compared to their planktonic counterparts [6]. Moreover, some chemical disinfectant treatments have also been discontinued due to their side effects of tissue damage or accidental injury caused by leakage [3]. Therefore, it is essential to develop effective root canal disinfection methods to improve the outcomes of endodontic infection treatment [7, 8].

Successful endodontic infection treatment requires an effective disinfectant technique such as photodynamic therapy (PDT) [7, 9, 10]. The reason that PDT has gained attention among other treatments is the fact that it not only disinfects the root canal, but also preserves or possibly improves the chemical/mechanical stability of the dentin. The principle of PDT is based on a nontoxic photosensitizer (PS) which is activated by specific wavelengths and forms cytotoxic reactive oxygen species (ROS) that can directly damage sub-cellular components [9-11]. The efficacy of PDT depends on the type, concentration, and incubation time of PS, and laser parameters including wavelength, power density and time of irradiation [9]. For PSs with a negative charge (i.e. anionic PSs) like indocyanine green (ICG), the reduced efficacy of PDT is mostly attributed to the reduced interaction between the PS and

cell the surface of negatively charged microorganisms which decrease the production of ROS during photoactivation [12].

In order to improve the binding of ICG to microorganisms, studies suggest development of nano-PS conjugates for photodynamic therapy [12, 13]. Recently, nano-graphene oxide (NGO), an oxidized derivative of graphene, has earned popularity in biomedical applications due to its high surface area, high functional groups and cost-effective large scale synthesis [13]. So, the objective of the current study was to improve ICG photodynamic properties through incorporation of ICG into NGO in order to produce NGO-ICG as a new PS and also to assess the antimicrobial effects of NGO-ICG against *E. faecalis* after photodynamic therapy by counting colony forming units (CFUs) and biofilm formation ability as a major virulence factor. By revealing a significant increase in antimicrobial properties of NGO-ICG compared to ICG against *E. faecalis*, at least in part, our findings might help devise strategies for effective adjuvant treatment of endodontic infections as well as other local oral infections.

2. Materials and Methods

2.1. Preparation of NGO

GO (Qingdao Tianhe Graphite Co. Ltd., Quingdao, China) was synthesized based on a modified Hummers method [14]. Graphite flakes were oxidized using a combination of powerful reagents, i.e. sulfuric acid (H_2SO_4, 99%), potassium persulfate ($K_2S_2O_8$), and phosphorus pentoxide (P_2O_5) (all were purchased from Sigma-Aldrich, St Louis, MO, USA). After that, GO powder was initially dispersed in dry toluene and then sonicated at room temperature (25±2 °C). Then, dispersed GO was treated with 3-aminopropyltriethoxysilane (APTES) in toluene under nitrogen atmosphere for 24 h at 110 °C. Finally, residual APTES was completely removed by repetitive toluene washing. The product was left to dry overnight in a vacuum drying oven (Thermo Napco vacuum Oven Model 5831., MA, USA) [15]. After that, NGO was transferred to the solution. Then, the precipitates were washed with distilled water and ethanol at 20 °C and finally dried in a vacuum desiccator [16].

2.2. Loading of ICG onto NGO-ICG

Loading of ICG (Serva, USA) onto NGO was performed according to the following: first, ICG (2 mg) was added to 5 mL NGO (2 mg/mL) and the suspension was stirred. The product was centrifuged at 6000 rpm for 10 min at 10 °C to remove unbound ICG molecules. The fabricated NGO-ICG material (Figure 1) was stored at 4 °C in the dark for further use [17].

2.3. Confirmation of synthesized NGO-ICG

Fourier Transform Infrared Spectroscopy (FT-IR) on a Magna-IR 750 FT-IR spectrometer (Nicolet, USA) was applied for confirmation of synthesized NGO-ICG. Characterization of multifunctional groups, and types of chemical bonds of the NGO-ICG, and general structure of NGO-ICG were confirmed by FT-IR and scanning electron microscopy (SEM).

2.4. Spectral analysis of NGO-ICG

Ultraviolet–visible (UV-Vis or UV/Vis) spectra were compared before and after loading ICG onto NGO (ICG vs NGO-ICG) using the UV-Vis spectrometer (Lambda 25, PerkinElmer, USA) for determination of spectral properties of ICG in the presence of GO.

2.5. Bacterial strain and culture conditions

In this study, the strain ATCC 29212 of *E. faecalis* was used. It was aerobically cultured in the fresh brain heart infusion (BHI) broth (Merck, Darmstadt, Germany) at 37 °C until the logarithmic growth phase was achieved (4–5 h). The cell density was adjusted in a spectrophotometer to a final concentration of 1.0×10^6 CFU/mL (optical density [OD] 600 nm: 0.2) [10].

2.6. Preparation of photosensitizer for ICG-PDT

In order to prepare an appropriate stock dilution of ICG (Serva, USA), 4 mg/mL ICG was dissolved in sterile distilled water and kept in dark conditions before use.

2.7. Light source

The 810 nm diode laser system (DX82, Konftec, Taiwan) with an output power of 250 mW was used for a period of 60 s on a surface of 0.384 cm^2 with a diameter of 6.39 mm as a light source for PDT experiments [18].

2.8. Study design

To evaluate the effect of PDT based on NGO-ICG and PDT based on ICG on virulence characteristics of *E. faecalis*, the test groups containing *E. faecalis* strains were subjected to:

A. ICG group (at final concentration of 1000 μg/mL)
B. ICG + Laser group (at final concentration of 1000 μg/mL of ICG + irradiation at an energy density of 31.2 J/cm^2)
C. NGO-ICG group (at an incorporated concentration of 200 μg/mL of ICG)
D. NGO-ICG + Laser group (at an incorporated concentration of 200 μg/mL of ICG + irradiation at an influence rate of 31.2 J/cm^2)
E. Control group: only bacterial suspension

2.9. Antimicrobial Photodynamic Therapy (aPDT)

2.9.1. Colony count assessment

The antimicrobial effect against *E. faecalis* was evaluated by the broth micro-dilution method in accordance with the Clinical and Laboratory Standards Institute (CLSI) [19] as described previously [10]. Panel A and B were used for the evaluation of the antimicrobial effect of the test group A and B, respectively. The wells of a 96-well round-bottomed sterile polystyrene microplate (TPP; Trasadingen, Switzerland) were filled (100 μL) with ICG at a final concentration of 1000 μg/mL and then 100 μL of the fresh bacterial suspension in 2X BHI broth (final concentration of 1.0×10^5 CFU/mL) was added to the wells. In panel C and D, 100 μL NGO-ICG (at a final concentration of 200 μg/mL of incorporated ICG) was added

to wells and then 100 µL of fresh bacterial suspension in the BHI broth (at a final concentration of 1.0×10^5 CFU/mL) was added to the wells. All panels had one column as the positive control (bacterial growth) and one column as the sterility control (without bacterial inoculation). All panels were incubated in the dark for 5 min at room temperature. After incubation, the panels B and D were irradiated using the diode laser 810 nm for 60 s in a continuous mode. Then, ten-fold serial dilutions (up to 10^{-5}) of the content of each well in all panels were prepared in phosphate-buffered saline (PBS; 10 mM Na2HPO4, 2 mM NaH2PO4, 2.7 mM KCl and 137 mMNaCl at pH 7.4). Samples (10 µL) from each dilution were placed on the BHI agar (Merck, Darmstadt, Germany) and spread over the entire agar surface with a sterile spreader (1:10 dilution). Ten µL of the positive control well was transferred and spread over a non-selective enriched nutrient agar (e.g., blood agar plates) for purity checkup.

To ensure that the column contained 2–8 × 10^5 CFU/mL bacteria (the acceptable range), 10 µL of the positive growth control was diluted with 1 mL saline (1:100 dilution) and mixed; then, 10 µL of the suspension was transferred to a non-selective agar medium (e.g. trypticase soy agar) and spread over the entire agar surface with a sterile spreader (1:100 dilution). The colony count plates and the purity plates were incubated at 37 °C for 24 h. The calculation of the colony count (CFUs/mL) of the test wells was done based on the method of Miles and Misra [20].

2.9.2 Assessment of biofilm formation ability in treated planktonic E. faecalis by crystal violet assay

The biofilm forming ability of *E. faecalis* was observed to be in agreement with a previous study [18]. The free-floating bacteria (150 µL aliquots) in planktonic suspension which were adjusted to a final concentration of 1.5×10^8 CFU/mL were placed in flat-bottomed microplates (TPP; Trasadingen, Switzerland). The anti-biofilm formation ability of each of the above groups A-E (study design) was evaluated as described previously [10]. After each treatment, the microplates were incubated at 37 °C for 24 h to allow biofilm formation. After pouring out the contents of the microplates and washing them with PBS, the remaining suspension of the wells containing free-floating planktonic bacteria was removed.

The biofilm was quantified in accordance with previous studies [6, 21-24]. In short, 200 µL of 0.1% (wt/vol) crystal violet was used to stain biofilm cells at room temperature (25 ±2 °C) for 15 min. After two rounds of PBS washing, the wells were treated with 95% ethanol at room temperature for 10 min and left to dry. In order to quantify the biofilms, the wells were filled with acetic acid (150 µL of 33% [vol/vol]) and the absorbance quantification was determined by a microplate reader (Thermo Fisher Scientific, US) at 570 nm. The biofilm formation was clarified according to the criteria mentioned in a previous study, [6].

2.10. Statistical Analysis

The results of the colony count measurements and biofilm formation assessment groups were statistically analyzed using the two-way analysis of variance (ANOVA) followed by Tukey's

test. All experiments were performed at least three times, and the results were reported as mean± standard deviation (SD). The significance level was set at 0.05.

3. Results

3.1. FT-IR and SEM analysis

FT-IR analysis confirmed the synthesis of NGO-ICG in this study. The FT-IR spectra of GO showed the characteristic peaks of GO at 3420 cm^{-1} (O–H st), 1740 cm^{-1} (C=O st), 1630 cm^{-1} (C=C st), 1221 cm^{-1} (C–O st) and 1074 cm^{-1} (C–O–C), confirming the successful formation of GO.

ICG was successfully conjugated to the surface of NGO according to indication of the stretching vibrations of S=O, C-S, and S-O (1074 cm^{-1}). Another confirmation for the loading of ICG was the presence of the vibrational stretching of C=N and C=C at 1644 cm^{-1} and 1424 cm^{-1} respectively, as well as the vibrational stretching of the single-bond C-N at 1356 cm^{-1}, which are all reported in ICG. As shown in Figure 2, the SEM image implied that the sheets that formed NGO-ICG were smooth with small wrinkles at the edges.

3.2. Spectral analysis of NGO-ICG

As shown in Figure 3, comparison of UV-Vis spectra before (the black line) and after ICG loading on NGO (the red dotted line) showed successful loading of ICG onto NGO. Comparison of the absorption spectrum of NGO (Figure 3; blue line) and the absorption spectrum of free ICG (Figure 3; black line) indicated that the ICG molecules were loaded on the surface of the NGO due to strong $\pi - \pi$ stacking and hydrophobic interactions. This effect was clearly shown in the NGO-ICG absorption spectrum (Figure 3; red line).

3.3. CFU count

NGO-ICG-PDT and ICG-PDT significantly reduced cell viability of *E. faecalis* by 2.81- and 1.91-log as compared to the control group (untreated bacteria; all $P < 0.05$; Figure 4) respectively, whereas there was no remarkable reduction in the bacterial population in NGO-ICG and ICG alone ($P > 0.05$). A significant difference was observed between the antimicrobial effect of NGO-ICG-PDT at a final concentration of 200 μg/mL of incorporated ICG and ICG-PDT at a final concentration of 1000 μg/mL of ICG (90.6- and 43.6- percent reduction in bacterial count, respectively; $P < 0.05$; Figure 4).

3.4. PDT reduced biofilm formation in E. faecalis by crystal violet assay

A 99.4 % and 78.2% reduction was observed in the ability of biofilm formation of *E. faecalis* for NGO-ICG-PDT and ICG-PDT respectively as compared with the control group ($P < 0.05$). Our results showed that biofilm formation of *E. faecalis* was not significantly reduced when the bacterial cells were treated with NGO-ICG and ICG alone ($P > 0.05$; Figure 5). The anti-biofilm potential of NGO-ICG-PDT at a lower final concentration of ICG (200 μg/mL) was 1.3 time more than the ICG-PDT at a higher final concentration of ICG (1000 μg/mL) ($P > 0.05$).

4. Discussion

Enterococcus faecalis is a significantly resistant endodontopathogenic bacterial species, and conventional disinfectant treatments only cause a partial reduction in this species [25]. The biofilm formation ability of *E. faecalis* is the most important factor involved in bacterial resistance to antimicrobial agents. Numerous *in vitro*, *ex vivo*, and *in vivo* studies using PDT indicate that this approach can potentially maximize biofilm microbial degradation [18, 23, 26].

The efficiency of PDT depends on several factors such as the type and concentration of PS, and energy dose and irradiation time of the light. There are important factors that make a PS ideal for PDT, including low levels of dark toxicity, high interaction with microbial cells, and the presence of absorption bands in the so-called optical window (600–900 nm) for sufficient tissue penetration of light [27]. ICG has received the Food and Drug Administration (FDA) approval for clinical applications and also has the near-infrared (NIR) absorption which is thought to be an effective PS against Gram-positive and Gram-negative oral bacteria [17]. However, several limitations of ICG molecules, such as concentration-dependent aggregation in aqueous solutions [17], low interaction with microbial cells, and poor delivery to the target site [28], lead to decreased efficiency of aPDT [11]. Therefore, the future of PDT largely depends on introducing more effective PSs. In addition to the photochemical processes, several factors are important in aPDT efficiency, such as targeting of microorganisms. [9].

Modifications to the ICG molecule in order to improve its photodynamic properties have been addressed in recent studies. A study showed that PDT based on nanochitosan (NC)-ICG, as a new PS, had significant antimicrobial effects against *Porphyromonas gingivalis* when compared to the ICG-PDT. While PDT based on ICG (500 μg/mL) did not cause any significant antimicrobial effect on *P. gingivalis*, application of the NC-ICG reduced the CFU/mL by two $\log_{10}$ for *P. gingivalis* [29]. It was revealed that the surface of NC-ICG was given a positive charge by a chitosan coating to improve its ability to adhere to the bacteria than the ICG [29]. Sasaki *et al*. [30] demonstrated that PDT that photosensitizes ICG-loaded nanospheres through the gingivae from outside the pocket using a diode laser has marked bactericidal effects against *P. gingivalis*, with reductions in colony-forming units of four $\log_{10}$ (99.99% reduction) compared with the control group. ICG-loaded nanospheres coated with chitosan (ICG-nano/c) demonstrate nano-spherization, positive charging of the chitosan coating of the PS, and improved antimicrobial effects of PDT [29]. Another *in vitro* study [31] showed that combination of Trolox™ antioxidant, a water soluble vitamin E analogue, with ICG significantly enhanced the antimicrobial effect of ICG up on irradiation with NIR-laser-light against different periodontopathogenic bacterial species. It is known that under hypoxic conditions, antioxidants can also serve as substrate for PSs of the excited triplet state, causing intense formation of superoxide radical anions and other ROS [32].

However, different studies have already indicated the enhancing character of GO in ICG-PDT treatment of neoplastic cells. For example, Ocsoy et al. [33] reported that aptamer-functionalized magnetic GO conjugates loaded with ICG resulted in a significant stronger photoinactivation of the human T-cell leukemia cell line (CCRF-CEM cells) compared to treatment without it. In another study, nanohybrid NGO-copper sulfide (CuS)/ICG was introduced as a NIR light activable theranostic nano-drug for deep-seated cancer noninvasive phototherapy [34]. Sharker et al. [35] synthesized a pH-dependent, NIR-sensitive, reduced

GO hybrid nano-composite via electrostatic interaction with ICG which markedly improved *in vitro* cancer cell targeted photothermal destruction compared to free ICG.

In this study, we designed and examined a nano-carrier (i.e. NGO) that conjugated with ICG (NGO-ICG) in order to increase the efficacy of PS during aPDT. To the best of our knowledge, this is the first study to investigate the antimicrobial effect of NGO-ICG as a new nano-PS in PDT. According our results, the antimicrobial potential of PDT based on NGO-ICG with a lower final concentration of ICG (200 μg/mL) was 47% more than the PDT based on ICG (1000 μg/mL) ($P < 0.05$). Also, in this study, the anti-biofilm potential of NGO-ICG-PDT at a lower final concentration of ICG (200 μg/mL) was 1.3 time more than ICG-PDT (1000 μg/mL) ($P > 0.05$). Our results showed that NGO-ICG was more effective for antimicrobial PDT when compared with ICG, which is consistent with previous reports, demonstrating that integration of the nanomaterials with strong intrinsic absorption in NIR region (e. g. graphene [36-38]) and PS in a single complex is becoming a promising strategy to combine photothermal (PTT) and PDT.

Furthermore GO has various properties that make it a promising material for ICG carrier substances [16]. The ultrahigh surface area of GO allows loading of many aromatic ICG molecules [17, 28]. Moreover, incorporation of ICG into GO nano-vehicles can significantly improve the stability and bioavailability effects of ICG, with distinctive therapeutic effects [39]. It is known that, singlet oxygen generation ($^1O_2$) is a key component for PDT [39]. Ocsoy et al. [39] demonstrated that the GO-ICG-PDT causes a $^1O_2$ increase greater than that of ICG-PDT. They demonstrated that ICG-GO conjugates offered enhanced PDT when irradiated with the 810 nm NIR laser by producing more singlet oxygen generation than that of ICG alone. Ocsoy *et al*. [33] showed that ICG solution exhibits a characteristic absorption peak around 780 nm. The authors reported that ICG aggregates in aqueous solution forms, and also degrades rapidly. After loading ICG on GO, an absorption peak of ICG-GO conjugates appears around 808 nm (28 nm red shift), which matches the NIR laser wavelength used for PDT. Therefore, GO can be used as both stabilizer and a carrier to prevent degradation and aggregation of ICG [33].

In this study, no significant differences were observed in the CFU/mL and biofilm formation between the groups treated with the PSs only (ICG and NGO-ICG) and the control group (untreated bacteria). These findings are consistent with the principles of PDT, suggesting that application of the PSs alone has no antimicrobial effect [9].Our finding showed that PDT with NGO-ICG had potential antimicrobial and anti-biofilm activities against *E. faecalis*. However, further investigations are required to identify the effect of NGO-ICG-material on the tooth color in *ex vivo* assays, the expression of virulence factors, and metabolic activity of *E. faecalis* as well as the other endodontopathogenic bacteria.

5. Conclusion

Although the concentration of the conjugated ICG in NGO-ICG, as a desirable platform, was one-fifth of its concentration in conventional PDT, it could significantly reduce the number of *E. faecalis*. The anti-biofilm activity of PDT based on NGO-ICG at a lower final concentration of ICG (one-fifth) was 1.3 times more effective than the PDT based on ICG. In conclusion, the use of this new NIR photo-triggered drug delivery system, in addition to its antimicrobial and anti-biofilm properties, has advantages like cost-effectiveness,

exposure to lower dye concentrations (less toxicity), and less discoloration of the teeth. NGO-ICG-PDT can be considered as an adjuvant to conventional irrigation for endodontic treatment which presumably improves the treatment outcome.

Conflict of interest

The authors declare that there is no conflict of interests regarding the publication of this paper.

Acknowledgement

This research has been supported by Laser Research Center of Dentistry (LRCD), Dentistry Research Institute, Tehran University of Medical Sciences & Health Services grant No. 96-02-97-35451.

References:

[1] R. Ng, F. Singh, D.A. Papamanou, X. Song, C. Patel, C. Holewa, et al., Endodontic photodynamic therapy *ex vivo*, JOE. 37 (2016) 217–222.

[2] D.E. Böttcher, N.T. Sehnem, F Montagner, C.C Fatturi Parolo, F.S Grecca, Evaluation of the Effect of *Enterococcus faecalis* Biofilm on the 2% Chlorhexidine Substantivity: An *in vitro* Study, JOE. 41 (2015) 1364–1370.

[3] C. Komine , Y. Tsujimoto, A Small Amount of Singlet Oxygen Generated via Excited Methylene Blue by Photodynamic Therapy Induces the Sterilization of *Enterococcus faecalis*, JOE. 39 (2013) 411–414.

[4] M. Barbosa-Ribeiro, A. De-Jesus-Soares, A.A. Zaia, C.C. Ferraz, J.F. Almeida, B.P. Gomes, Antimicrobial susceptibility and characterization of virulence genes of *Enterococcus faecalis* isolates from teeth with failure of the endodontic treatment, JOE. 42 (2016) 1022–1028.

[5] M. Pourhajibagher, A. Bahador, Is antimicrobial agents can considered as effective weapons against endodontic infections by *Enterococcus faecalis*?, Der. Pharma. Chemica. 7 (2015) 196-200.

[6] M. Pourhajibagher, M. Mokhtaran, D. Esmaeili, A. Bahador, Assessment of biofilm formation among *Acinetobacter baumannii* strains isolated from burned patients, Der. Pharma. Lett. 8 (2016) 108-112.

[7] V. Chrepa , G.A. Kotsakis, T.C. Pagonis , K.M. Hargreaves, The effect of photodynamic therapy in root Canal disinfection: A systematic review, JOE. 40 (2014) 891–898.

[8] A. Persadmehr , C.D. Torneck , D.G. Cvitkovitch , V. Pinto, I. Talior , M. Kazembe, et al., Bioactive chitosan nanoparticles and photodynamic therapy inhibit collagen degradation *in vitro*, JOE. 40 (2014) 703–709.

[9] N. Chiniforush, M. Pourhajibagher, S. Shahabi, A. Bahador, Clinical approach of high technology techniques for control and elimination of endodontic microbiota, J. Laser Med. Sci. 6 (2015) 139–150.

[10] M. Pourhajibagher, N. Chiniforush, S. Shahabi, R. Ghorbanzadeh, A. Bahador, Sub-lethal doses of photodynamic therapy affect biofilm formation ability and metabolic activity of *Enterococcus faecalis*, Photodiagn. Photodyn. Ther. 15 (2016) 159–166.

[11] T. Rödig, S. Endres, F. Konietschke, O. Zimmermann, H.G. Sydow, A. Wiegand, Effect of fiber insertion depth on antimicrobial efficacy of photodynamic therapy against *Enterococcus faecalis* in root canals, Clin. Oral. Invest. 21 (2017) 1753–1759.

[12] A. Shrestha, A. Kishen A, Antibiofilm efficacy of photosensitizer-functionalized bioactive nanoparticles on multispecies biofilm, JOE. 40 (2014) 1604–1610.

[13] Y.W. Wang, Y.Y. Fu, Q. Peng, Sh.Sh. Guo, G. Liu, J. Li, et al., Dye-enhanced graphene oxide for photothermal therapy and photoacoustic imaging, J. Mater. Chem. B. 1 (2013) 5762–5767.

[14] C. Pak, D.C. Lee, Crystalline transformation of colloidal nanoparticles on Graphene Oxide, 4 (2012) 1021–1029.

[15] A. Kumar, B. Behera, S.S. Ray, Microwave-assisted surface-initiated redox polymerization of acrylamide with functionalized graphene oxide for aqueous lubricant additive, RSC. Adv. 5 (2015) 39474–39481.

[16] X. Yang, Y. Wang, X. Huang, Y. Ma, Y. Huang, R. Yang, et al., Multi-functionalized graphene oxide based anticancer drug-carrier with dual-targeting function and pH-sensitivity, J. Mater. Chem. 21(2011) 3448–3454.

[17] J. Chen, C. Liu, G. Zeng, Y. You, H. Wang, X. Gong, et al., Indocyanine green loaded reduced Graphene Oxide for *in vivo* photoacoustic/fluorescence dual-modality tumor imaging, Nanoscale. Res. Lett. 11 (2016) 85.

[18] N. Chiniforush, M. Pourhajibagher, S. Parker, S. Shahabi, A. Bahador, The in vitro effect of antimicrobial photodynamic therapy with indocyanine green on *Enterococcus faecalis*: Influence of a washing vs non-washing procedure, Photodiagnosis. Photodyn. Ther. 16 (2016) 119–123.

[19] Methods for Dilution Antimicrobial Tests for Bacteria That Grow Aerobically:Approved Standard, Clinical and Laboratory Standards Institute, Wayne, PA, 2015.

[20] A.A. Miles, S.S. Misra, The estimation of bactericidal power of the blood, J. Hyg. (Lond.) 38 (1938) 732.

[21] M. Pourhajibagher, E. Boluki, N. Chiniforush, B. Pourakbari, Z. Farshadzadeh, R. Ghorbanzadeh, et al., Modulation of virulence in *Acinetobacter baumannii* cells surviving photodynamic treatment with toluidine blue, Photodiagn. Photodyn. Ther. 15 (2016) 202–212.

[22] M. Pourhajibagher, N. Chiniforush, R. Ghorbanzadeh, A. Bahador, Photo-activated disinfection based on indocyanine green against cell viability and biofilm formation of *Porphyromonas gingivalis*, Photodiagn. Photodyn. Ther. (2016) 30180–30185.

[23] M. Pourhajibagher, N. Chiniforush, S. Shahabi, R. Ghorbanzadeh, A. Bahador, Sublethal doses of photodynamic therapy affect biofilm formation ability and metabolic activity of *Enterococcus faecalis*, Photodiagn. Photodyn. Ther. 15 (2016) 159–166.

[24] M. Pourhajibagher, N. Chiniforush, R. Raoofian, R. Ghorbanzadeh, S. Shahabi, A. Bahador, Effects of sub-lethal doses of photo-activated disinfection against *Porphyromonas gingivalis* for pharmaceutical treatment of periodontal-endodontic lesions, Photodiagn. Photodyn. Ther. 16 (2016) 50–53.

[25] S. Kranz, A. Guellmar, A. Völpel, B. Gitter, V. Albrecht, B.W Sigusch, Photodynamic suppression of *Enterococcus faecalis* using the photosensitizer mTHPC, Lasers. Surg. Med. 43 (2011) 241–248.

[26] L.A. Silva, A.B. Jr Novaes, R.R. de Oliveira, P. Nelson-Filho , M.Jr. Santamaria , R.A Silva, Antimicrobial photodynamic therapy for the treatment of teeth with apical periodontitis: A histopathological evaluation, JOE. 38 (2012) 360–366.

[27] F.F. Sperandio, Y.Y. Huang, M.R. Hamblin, Antimicrobial photodynamic therapy to kill Gram-negative bacteria, Recent. Pat. Antiinfect. Drug. Discov. 8 (2013) 108-120.

[28] B. Yan, H. Qin, Indocyanine green loaded graphene oxide for high-effcient photoacoustic tumor therapy, J. Innov. Opt. Health Sci. 9 (2016) 164200.

[29] A. Nagahara, A. Mitani, M. Fukuda, H. Yamamoto, K. Tahara, I. Morita, et al., Antimicrobial photodynamic therapy using a diode laser with a potential new photosensitizer,

indocyanine green-loaded nanospheres, may be effective for the clearance of *Porphyromonas gingivalis*, J. Periodontal. Res. 48 (2013) 591-599.

[30] Y. Sasaki, J.I. Hayashi, T. Fujimura, Y. Iwamura, G. Yamamoto, E. Nishida, et al., New Irradiation Method with Indocyanine Green-Loaded Nanospheres for Inactivating Periodontal Pathogens, Int. J. Mol. Sci. 18 (2017) doi: 10.3390/ijms18010154.

[31] S. Kranz, M. Huebsch, A. Guellmar, A. Voelpel, S. Tonndorf-Martini, B.W. Sigusch, Antimicrobial photodynamic treatment of periodontopathogenic bacteria with indocyanine green and near-infrared laser light enhanced by Trolox (TM), Lasers. Surg. Med. 47 (2015) 350-360.

[32] J. Jakus, O. Farkas, Photosensitizers and antioxidants: a wayto new drugs?, Photochem. Photobiol. Sci. 4 (2005) 694–698.

[33] I. Ocsoy, N. Isiklan, S. Cansiz, N. Özdemir, W. Tan, ICG-conjugated Magnetic Graphene Oxide for Dual Photothermal and Photodynamic Therapy, RSC. Adv. 6 (2016) 30285-30292.

[34] C. Wu, A. Zhu, D. Li, L. Wang, H. Yang, H. Zeng, Y. Liu, Photosensitizer-assembled PEGylated graphene-copper sulfide nanohybrids as a synergistic near-infrared phototherapeutic agent, Expert. Opin. Drug. Deliv. 13 (2016) 155-165.

[35] S.M. Sharker, J.E. Lee, S.H. Kim, J.H. Jeong, I. In, H. Lee, et al., pH triggered in vivo photothermal therapy and fluorescence nanoplatform of cancer based on responsive polymer-indocyanine green integrated reduced graphene oxide, Biomaterials. 61 (2015) 229-238.

[36] Y Wang, H .Wang, D. Liu, S. Song, X. Wang, H. Zhang, Graphene oxide covalently grafted upconversion nanoparticles for combined NIR mediated imaging and photothermal/photodynamic cancer therapy, Biomaterials. 34 (2013) 7715–7724.

[37] Z. Hu, F. Zhao, Y. Wang, Y. Huang, L. Chen, N. Li, et al., Facile fabrication of a C60-polydopamine-graphene nanohybrid for single light induced photothermal and photodynamic therapy, Chem. Commun. (Camb). 50 (2014) 10815–10818.

[38] A. Sahu, W.I. Choi, J.H. Lee, G. Tae, Graphene oxide mediated delivery of methylene blue for combined photodynamic and photothermal therapy, Biomaterials. 34 (2013) 6239–6248.

[39] Y. Li, H. Dong, Y. Li, D. Shi, Graphene-based nanovehicles for photodynamic medical therapy, Int. J. Nanomedicine. 10 (2015) 2451–2459.

Figure legends:

Figure 1. Schematic of the chemical path to the synthesis of NGO-ICG. Abbreviations: GO, graphen oxid; APTES, 3-aminopropyltriethoxysilane; EDC, 1-ethyl-3-(3-dimethylaminopropyl) carbodiimide; NHS, N-hydroxy succinimide; ICG, indocyanine green.

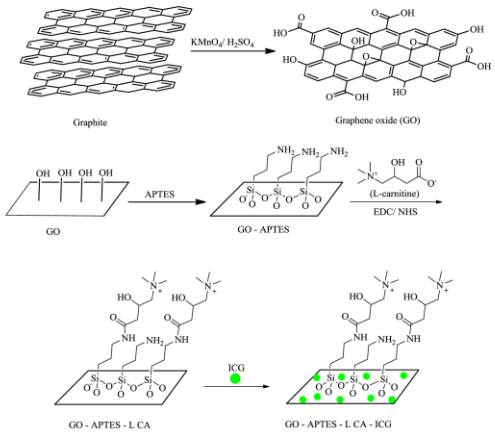

Figure 2. Scanning Electron Microscopy image shows the smooth sheets of NGO-ICG with small wrinkles at the edges.

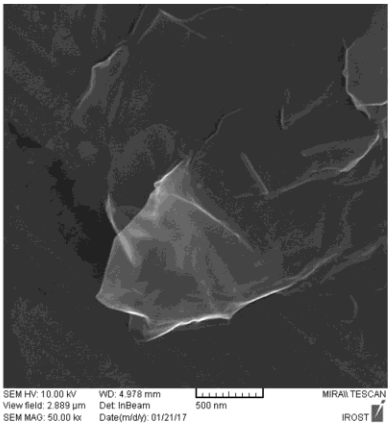

Figure 3. The comparison of the absorption spectrum of the GO (blue line) and the absorption spectrum of the free ICG (black line) at 780 nm indicates that the ICG molecules are loaded onto the surface of the GO due to strong π –π stacking and hydrophobic interactions. This effect is clearly shown in the GO-ICG absorption spectrum (red line).

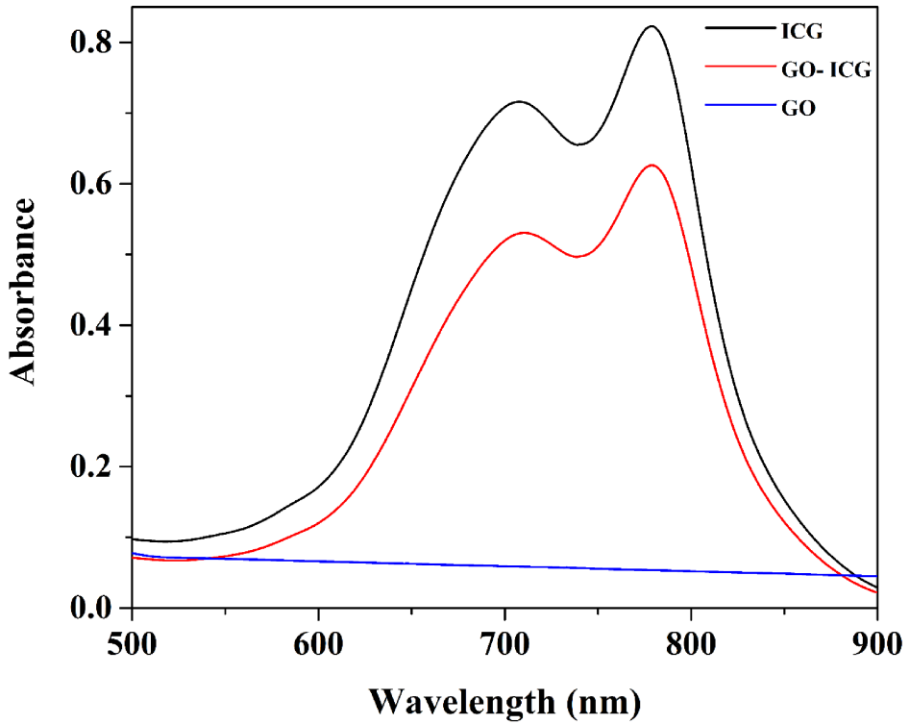

Figure 4. Effects of ICG-PDT and NGO-ICG-PDT on reduction of CFU/mL of *Enterococcus faecalis*. *Significantly different from the control, $P < 0.05$.

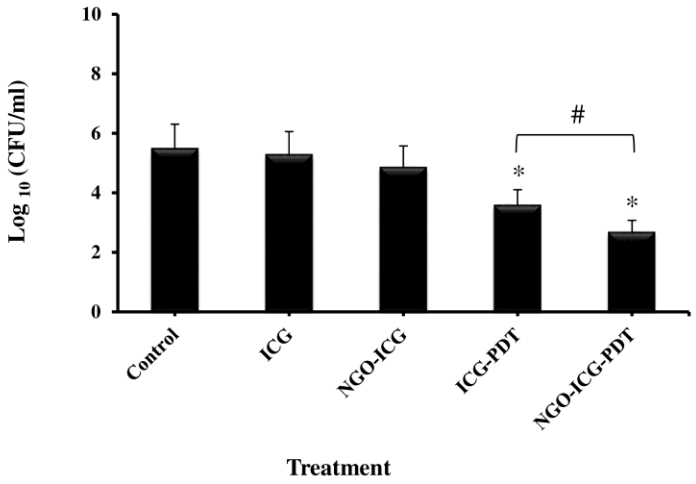

Figure 5. Effects of ICG-PDT and NGO-ICG-PDT on inhibition of biofilm formation ability of *Enterococcus faecalis*. *Significantly different from the control, $P < 0.05$.